

Restoration of Images from MIP of Chandrayaan-1

Preeti Panjwani, Arvind K. Singh, B. Gopala Krishna
 Satellite Photogrammetry and Digital Cartography Group
 Space Applications Centre (ISRO), Ahmedabad-380015
 {preeti_p, aksingh, bgk}@sac.isro.gov.in

Abstract— Chandrayaan-1, India's first mission to moon was launched on 22nd Oct 2008. It carried a Moon Impact Probe which impacted the moon's surface on 14 Nov 2008. MIP had an imaging camera called Moon Imaging System (MIS) to take the pictures of moon's surface while descending. All the images taken during flight were observed to have a certain kind of periodic impulse noise.

The present paper describes the approaches used to restore MIS images which include characterization of noise. Restoration of images is attempted in spatial as well as in frequency domain. Frequency domain restoration turned out to be better in terms of noise cleaning while retaining sharpness of the images.

Keywords-MIP, Chandrayaan-1, Image Restoration, Spatial domain filtering, Frequency Domain Filtering

I. INTRODUCTION

The Indian mission to moon Chandrayaan-1, lunar remote sensing orbiter was launched on 22nd October 2008. Chandrayaan-1 carried 11 scientific payloads out of which five were indigenously developed by India. One of them was the Moon Impact Probe (MIP) which impacted on the lunar surface on 14th November '08.

MIP contained three payloads viz. Radar Altimeter, Mass Spectrometer and the Moon Imaging System (MIS) [1]. Radar Altimeter was used to measure the altitude of the MIP during the descent on to the moon surface. Mass Spectrometer was used for measuring the constituents of tenuous lunar atmosphere and MIS for acquiring images of the surface of the moon at a close range during descent of the MIP. A schematic is shown in Figure 1 depicting MIP position (and MIS imaging) with respect to the mother ship Chandrayaan-1.

The data from MIS was received in Y, C_b, C_r format on ground. On careful examination of the images, a certain kind of periodic uniform noise is seen, which can be attributed to acquisition or transmission. Due to this noise, the images were not usable for applications such as target recognition, high resolution movie and registration with moon globe created by Clementine data [2]. Therefore restoration was required to use them properly for an application.

The purpose of the present work is to identify the restoration technique best suited to restore all the images from the above noise patterns.

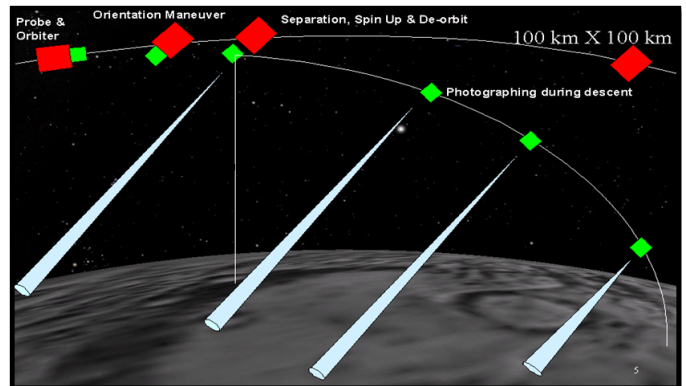


Figure 1. Detachment of MIP from the mother satellite i.e. Chandrayaan-1

II. DATA FROM MIS

MIS had an analog CCD video camera which took pictures in RGB format with the size of 576 × 720 (scan x pixel). For the purpose of transmission, images are converted into Y, C_b, C_r format, by separating luminance from the color information. The images acquired in terms of odd and even frames separated by 20 ms are used for the present analysis. These images are of the size 288 × 720 (scan × pixels).

On observing image data received from MIS, an interference pattern was seen in the image which is, in addition to the motion blur, due to the camera spin during imaging. The blur in the images was insignificant to the extent of affecting the image quality [3]. However the noise was major component, which affected the quality. Periodic noise patterns were observed in all the images which seemed to be space invariant. Though the cause of this noise is not known; usually periodic noise in an image arises from electrical and electrochemical interference during image acquisition.

III. RESTORATION METHODOLOGY

The image restoration techniques can be categorized in two different ways viz., spatial domain techniques and frequency domain techniques. The spatial domain techniques involve

direct manipulation of image pixels in image plane itself whereas frequency domain techniques are based on modifying the Fourier transform of the image [4][5].

The restoration process of an image can be modeled by a degradation function that together with an additive noise term, operates on an input image $f(x, y)$ to produce a degraded image $g(x, y)$. Given $g(x, y)$, some knowledge of the degradation function H and the additive noise term $n(x, y)$, the objective of the restoration is to obtain an estimate $\hat{e}(x, y)$ as close as possible to the original image $f(x, y)$.

$$g(x, y) = h(x, y) * f(x, y) + n(x, y), \text{ where } h(x, y) \text{ is the spatial representation of degradation function } H [3].$$

In case of MIS images, since the images are corrupted by salt and pepper additive noise and there is no knowledge available for the degradation function $h(x, y)$, the restoration is performed for the additive noise only.

IV. DATA SETS

Around 3000 frames were obtained from MIP during its journey to moon's surface. One of the MIP frames (Y component) is shown in the figure-2 below. The rectangle drawn in the image portion is used to show the comparison of original and restored image

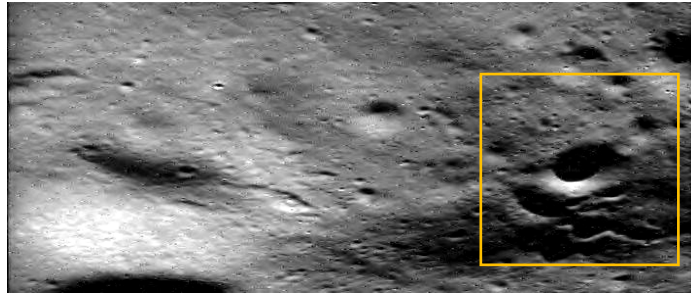


Figure 2. A frame from MIS

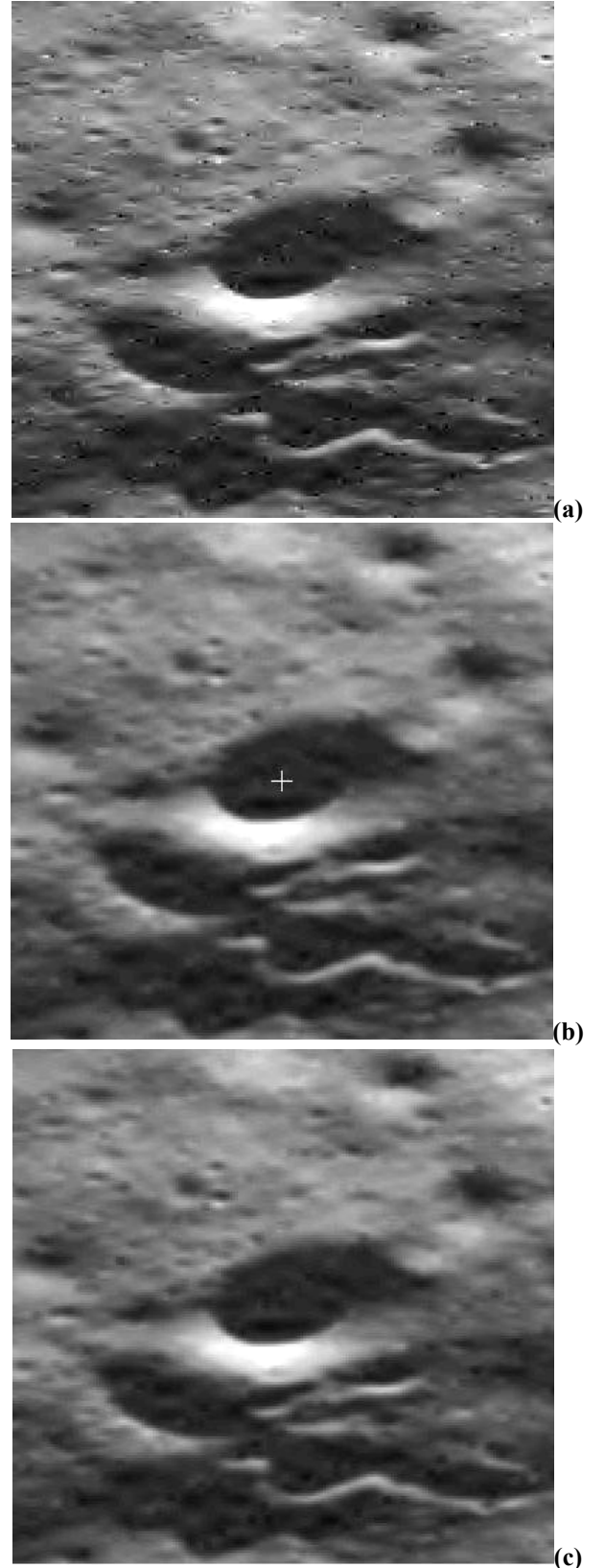
V. RESULTS

A. Restoration in spatial domain

In the first case, basic spatial domain filters which are mean, geometric mean, median and adaptive median filters have been used as they are easier to apply. The results obtained have been compared with the original images and analyzed both quantitatively and qualitatively. Figure 3 presents qualitative results for spatial domain filtering.

Results presented in Figure 3 show that mean and geometric mean filters remove noise but image features also get smoothed which introduces blur in the image, whereas median filter produces less smoothing compared to mean filters. Since both these filters affect all the pixels of the image uniformly, they blur the noise along with image detail also. Hence, the next technique applied is the adaptive median filter that tries to affect only the noise, retaining much of the image detail which can be observed in the result. But still the image

is not found to be satisfactory in terms of visual quality. Due to the residual noise left, the image was analyzed in frequency domain as the next step.



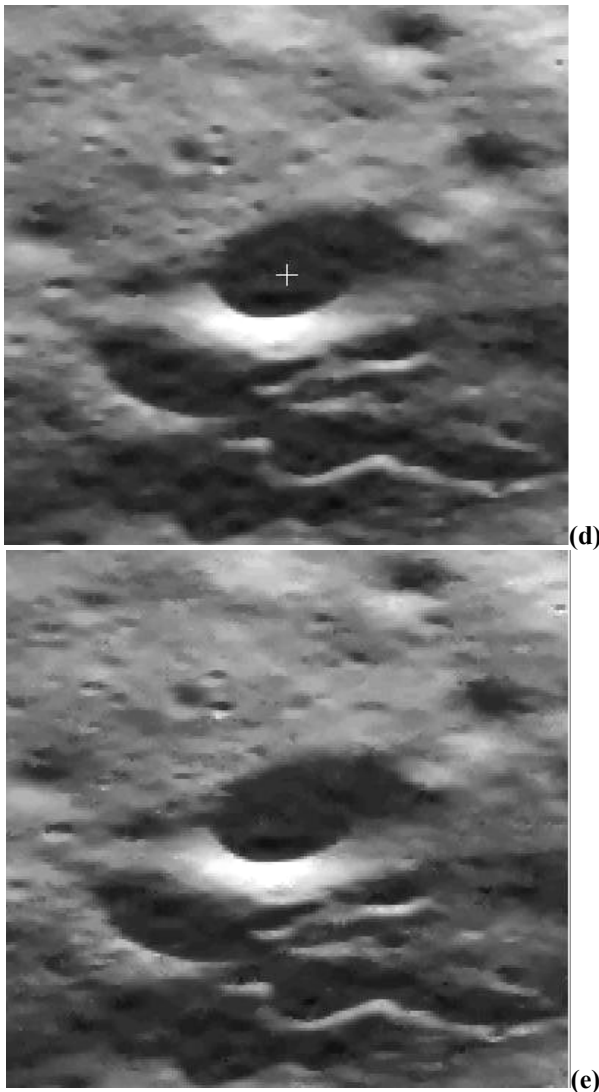


Figure 3. (a) Original Image (zoom 2x) (b) Simple Mean filtering (c) Geometric mean filtering (d) Median filtering (e) Adaptive median filtering

B. Restoration in frequency domain

Figure 4 below represents the Fourier transform of the image given in Figure 2. On observing Figure 4, it is seen that most of the image frequencies are concentrated at the center and the noise is seen as peaks following a particular pattern. Hence, a low pass filter can be a better option to restore the image. Further the strong peaks within the low pass filter support are eliminated through constructing a notch reject filter at each peak. First, an elliptical Butterworth low pass filter (EBLPF) was applied. The reason to apply Butterworth filter is that it has a smooth transfer function which does not produce a sharp cutoff between passed and filtered frequencies. The elliptical shape is chosen as the concentration of image frequencies is different for X and Y axis.

The image representation of transfer function of Elliptical Butterworth filter of order 2 is given in the Figure 5.

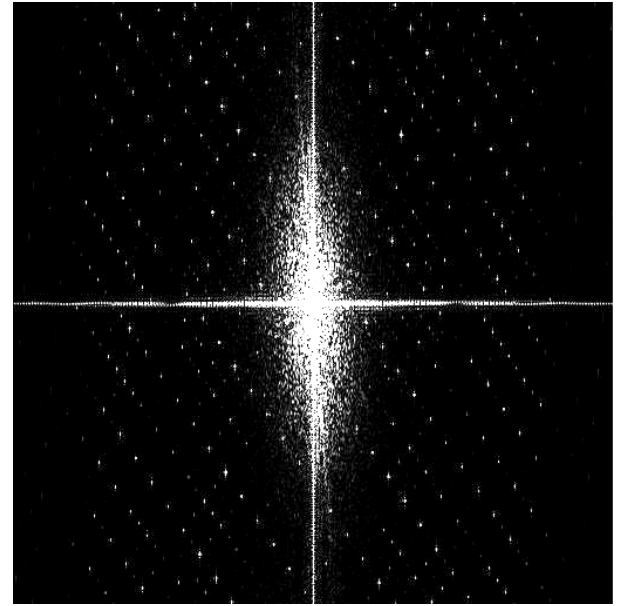


Figure 4. Fourier transform of the image

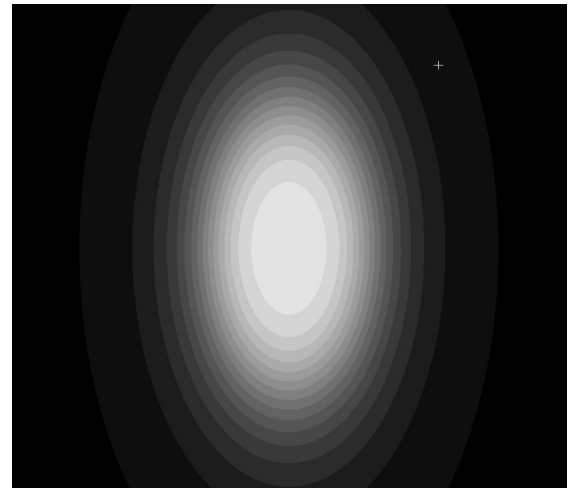


Figure 5. EBLPF transfer function

The result of applying EBLPF is shown in Figure 6. On observing Figure 6, in 2x zoom, some interference was still seen. Therefore, after applying EBLPF, the locations of noise peaks in the Fourier transform were identified by interactively observing the Fourier spectrum and notch reject filter was applied at those locations. The result of applying notch reject filter along with elliptical Butterworth low pass filter is shown in Figure 7.

From the result in Figure 7, it is observed that the noise has reduced to a significant level while the image details are also retained. Compared to spatial domain results, the image is sharper in this case and the extent of blurring is very less.

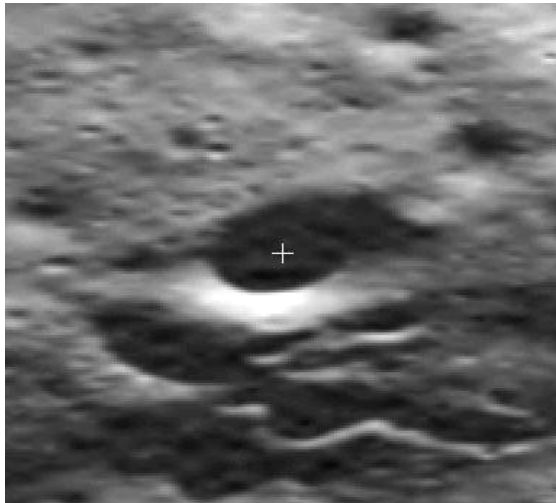


Figure 6. EBLPF applied image



Figure 7. Result of applying EBLPF along with notch reject filter

VI. NOISE ESTIMATION

The difference between the given image and restored image has been taken to see the amount of additive noise removed.

It is clear from Figures 8 and 9, that more image features are affected in spatial domain filtering as compared to frequency domain filtering as expected. Frequency domain separates image frequencies and noise frequencies in a much better way and hence provides control to remove noise frequencies in a much better way.

VII. QUANTITATIVE ANALYSIS OF RESULTS

For analyzing the results quantitatively, three segments were selected from the resulting images such that they cover full range of gray values. viz., one with very low gray values (dark region), other with medium gray values (average brightness) and the third having high gray values (bright region). The

results in terms of statistical parameters, mean and standard deviation (SD) are presented for one frame only. The segments selected are of size (10 x 10), with homogeneity in mind. The quantitative parameters are presented in the Table I.

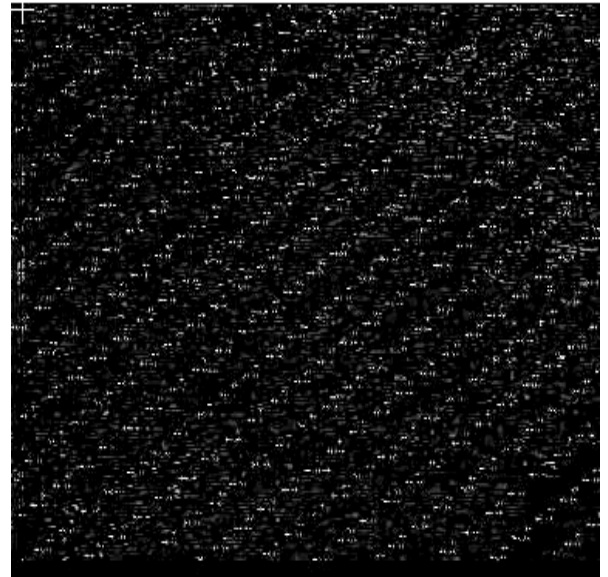


Figure 8. Noise estimation using spatial domain

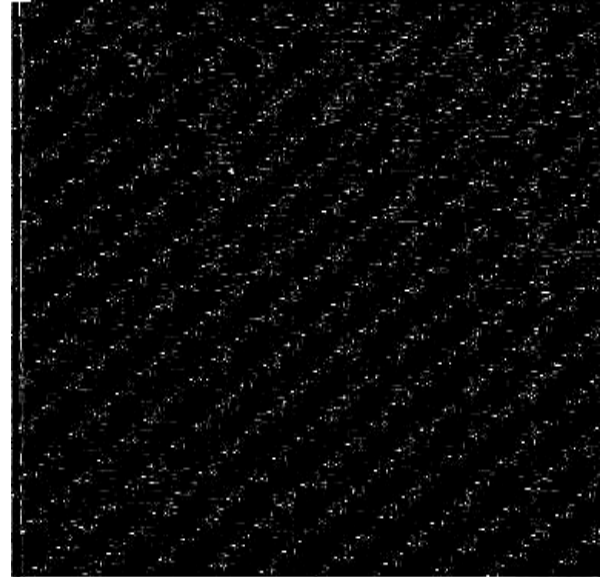


Figure 9. Noise Estimation using frequency domain filtering

The table shows decrease in SD compared to the original image for all the filters which indicates the reduction in noise at large. Mean filter averages the neighboring pixel values due to which the mean and standard deviation decreases marginally. Median filter replaces the values with local median which also results in decrease in mean and decrease in SD. Similar trend is seen even in adaptive median filter. In case of EBLPF and combination of EBLPF & Notch filter, the decrease in SD w.r.t. original is less as compared to spatial

filters. This is due to the fact that here, particular noise frequencies are targeted which retains more image details. The quantitative results indicate that smoothening has been performed by the filters though subjective verification gives the proof for best filter. In all the cases maximum count is decreased from the original and minimum is increased as expected due to the smoothening.

VIII. CONCLUSION AND FUTURE SCOPE

The images from MIS showed periodic impulse noise. Filters for noise removal are studied in spatial and frequency domains and were applied on these images.

Spatial domain techniques include mean, geometric mean, median and adaptive median filter, which are suitable for additive noise removal. On application, spatial domain techniques tend to smooth the image. Image features also get blurred along with noise. Median and adaptive median filters produce less blurring than mean and geometric mean filters. In frequency domain, noise is characterized through the Fourier transform. Low pass Butterworth filter of elliptical shape was first chosen to reject most of the noise frequencies. Remaining noise frequencies were identified and notch reject filters were applied to restore the image.

Results from both the techniques are compared and analyzed. Quantitative measures viz., mean and standard deviation on sample areas are studied and they are found to be following expected trends with respect to the smoothening. Frequency domain filters produce better results compared to spatial domain. This is due to the better characterization of noise possible through the Fourier transform. Hence, image features are less affected in case of frequency domain.

The quality of the resultant images is adequate (qualitatively) for further applications like creating a movie or overlaying on Clementine imagery or for mosaicing to create a larger path of MIP on moon surface.

Usage of notch filter is not ideal for periodic noise removal, where noise and image frequencies are mixed (in the low frequency range); image components are also removed along with the noise components. In future, optimum notch filtering is planned to be implemented to achieve greater accuracy in

image restoration. Optimum notch filtering is a combination of both i.e. frequency and spatial domain technique. The procedure consists of first isolating the principal contribution of the interference pattern and then subtracting a variable, weighted portion of the interference pattern from the corrupted image [4].

ACKNOWLEDGMENTS

The authors thankfully acknowledge the keen interest, encouragement and support received from Dr. R. R. Navalgund, Director, Space Applications Centre (SAC), Ahmedabad and Sri A. S. Kiran Kumar, Associate Director, SAC for this activity. Authors express their special thanks to Dr. P K Srivastava, Deputy Director (DD), Signal and Image Processing Area (SIPA) of SAC for his inspiration and keen interest in this work. Authors are indebted to Sri D. R. M. Samudraiah, DD, SEDA/SAC, Sri Sandip Paul, Head, SFED/SEG/SEDA/SAC, Dr. J. S. Parihar, DD, EPSA/SAC and Dr. M. Chakraborty, GD, ATDG/EPSA for their critical reviews and suggestions. Last but not the least; authors gratefully acknowledge the useful discussions held with Satellite Photogrammetry & Digital Cartography Group (SPDCG) members and Chandrayaan-1 DP team especially Mr. K Suresh and Mr. Ajay Parashar. Special thanks are also due to MIP project team led by Shri. Ashok Kumar from VSSC for their support in the initial discussions and providing the required information for understanding the MIS imagery.

REFERENCES

- [1] MIP Ground Segment Configuration and Design documents, MIP Team, VSSC, ISRO, 2007 (Vol. 6).
- [2] <http://webgis.wr.usgs.gov>
- [3] CHANDRAYAAN-1 GROUND SEGMENT - Critical Design Review Document for Payload Data Processing and Quality Evaluation Software, SAC Elements Volume 4-D GSSC-CH1/TR/20 Version 1.0, Dec. 2007
- [4] Digital Image Processing by Gonzalez & Woods, Prentice Hall, 2006.
- [5] Handbook of pattern recognition and image processing by Young and Tzay Y, Orlando Publications, 1986.

TABLE I. QUANTITAIVE PARAMETERS FOR DIFFERENT FILTERS

| | Brighter region | | | | | | | Average Brightness Region | | | | | | | Dark Region | | | | | | |
|-------------|-----------------|-------------|----------------|--------|-----------------|-------|---------------|---------------------------|-------------|----------------|--------|-----------------|-------|---------------|----------------|-------------|----------------|--------|-----------------|-------|---------------|
| | Original Image | Mean Filter | Geometric Mean | Median | Adaptive Median | EBLPF | EBLPF + Notch | Original Image | Mean Filter | Geometric Mean | Median | Adaptive Median | EBLPF | EBLPF + Notch | Original Image | Mean Filter | Geometric Mean | Median | Adaptive Median | EBLPF | EBLPF + Notch |
| Max | 106 | 97 | 97 | 97 | 97 | 98 | 97 | 66 | 60 | 59 | 61 | 60 | 60 | 61 | 21 | 18 | 18 | 19 | 19 | 19 | 19 |
| Min | 54 | 60 | 59 | 59 | 57 | 56 | 55 | 46 | 51 | 51 | 52 | 52 | 50 | 51 | 12 | 15 | 15 | 16 | 16 | 15 | 16 |
| Mean | 85.9 | 84.7 | 84.4 | 85.8 | 85.7 | 85.3 | 85.4 | 55.9 | 55.4 | 55.3 | 56.0 | 55.9 | 55.4 | 55.5 | 17.5 | 17.1 | 17.0 | 17.6 | 17.6 | 17.0 | 17.2 |
| SD | 11.4 | 10.2 | 10.5 | 10.6 | 10.7 | 11.0 | 11.1 | 3.0 | 2.2 | 2.2 | 2.3 | 2.3 | 2.4 | 2.5 | 1.4 | 0.7 | 0.7 | 0.7 | 0.6 | 0.8 | 0.7 |